A Study Of A New Class Of Discrete Nonlinear Schrödinger Equations

K. Kundu
Institute of Physics, Bhubaneswar 751005, India.
(Dated: February 8, 2008)

A new class of 1D discrete nonlinear Schrödinger Hamiltonians with tunable nonlinerities is introduced, which includes the integrable Ablowitz-Ladik system as a limit. A new subset of equations, which are derived from these Hamiltonians using a generalized definition of Poisson brackets, and collectively refered to as the N-AL equation, is studied. The symmetry properties of the equation are discussed. These equations are shown to possess propagating localized solutions, having the continuous translational symmetry of the one-soliton solution of the Ablowitz-Ladik nonlinear Schrödinger equation. The N-AL systems are shown to be suitable to study the combined effect of the dynamical imbalance of nonlinearity and dispersion and the Peierls-Nabarro potential, arising from the lattice discreteness, on the propagating solitary wave like profiles. A perturbative analysis shows that the N-AL systems can have discrete breather solutions, due to the presence of saddle center bifurcations in phase portraits. The unstaggered localized states are shown to have positive effective mass. On the other hand, large width but small amplitude staggered localized states have negative effective mass. The collison dynamics of two colliding solitary wave profiles are studied numerically. Notwithstanding colliding solitary wave profiles are seen to exhibit nontrivial nonsolitonic interactions, certain universal features are observed in the collison dynamics. Future scopes of this work and possible applications of the N-AL systems are discussed.

PACS numbers: 05.45.Yv, 05.60.Cd, 52.35.Mw, 63.20.Ls, 63.20.Pw

I. INTRODUCTION

As is well known, different nonlinear models can possess spatially localized solutions for solitary waves[1, 2, 3]. In many cases, the solitary waves are analyzed in the frame work of integrable models which, however, describe realistic physical systems with certain approximations[4]. Two important examples of integrable nonlinear equations are the nonlinear Schrödinger (NLS) equation, and the sine-Gordon (s-G) equation. While the first one is known to form "dynamical solitons", the last one yields "kink" and "antikink" solutions. These are also called "topological solitons"[1]. Dynamical solitons arise from the acute balance of nonlinearity and dispersion. The origin of topological solitons is the balance of nonlinearity and constraints from topological invariants[1, 5]. Along side these continuous equations, a pioneering example of integrable discrete differential equation is the Ablowitz-Ladik equation. This is often referred to as the integrable discretization of continuous NLS (ALDNLSE)[6, 7, 8]. On the other hand, the standard discretization of NLS gives the nonintegrable discrete nonlinear Schrödinger equation (DNLSE)[9, 10, 11].

The application of these continuous integrable equations in physics is quite extensive. The NLS, which has both dark and bright solitons, was first used to understand self-focussing and self-defocussing of carrier waves[12]. This equation later made inroads in the field of biological energy transport in the guise of "Davydov's soliton"[2, 13, 14, 15]. Quite recently, the NLS is investigated in relation to other phenomena, like Bose-Einstein condensates in standing waves, discrete solitons and breathers with dilute Bose-Einstein condensates, and the formation of unstable solitonic complexes[16, 17]. The mathematically very rich s-G equation has also many applications[1, 2]. It is used as a model for the propagation of dislocation in crystals and also for the propagation of magnetic flux in a long Josephson junction transmission line[1, 2]. On the other hand, the utility of the ALDNLSE in the analysis of physical problems is rather tortuous. Consider for example, physically motivated models, such as coupled nonlinear atomic strings with onsite or intersite anharmonic potentials[18], array of coupled optical waveguides[19], proton dynamics in hydrogen-bonded chains[4, 14, 20, 21], the Davydov and Holstein models(DHM) for transport in biophysical systems[2, 4, 21], and so on. In these models, either the ALDNLSE does not appear at all or it does not appear in its pristine form. However, to study the soliton dynamics perturbatively in these models, the ALDNLSE is the appropriate choice for the zeroth order approximation[18, 19, 21, 22]. This clearly shows that the ALDNLSE is an equation of great deal of significance in nonlinear science. For other applications of this equation we mention the following examples. The dynamics of low frequency and high frequency intrinsic localized modes in nonlinear lattices can be described to a good approximation by the ALDNLSE[23, 24]. Again, in the study of dark and bright excitons in systems with exchange and dipole-dipole interactions, it is shown that in some limiting cases the evolution equations resulting from model Hamiltonians are reduced to the exactly integrable ALDNLSE[25]. As another example, we cite the one-dimensional Frölich model of exciton(vibron)-phonon interaction. This model can be approximated by the ALDNLSE, provided we are interested in the dy-

namics of large width and small amplitude dynamical solitons[21]. One other important use of the ALDNLSE lies in the numerical integration of the NLS. This is done to avoid any numerical instability problem[6].

Any small perturbation may break the integrability so strongly that solitary waves can be unstable and in the extreme case may altogether disappear. The nonintegrablity in an otherwise integrable nonlinear equation can also give birth to internal modes, often called "shape modes" in solitary waves. These internal modes can drastically modify the soliton dynamics[26]. The physical origin of integrability breaking terms can be many. For example, this type of terms can arise from taking into consideration the effect of thermal fluctuations and the possible absence of order in the system[8, 27, 28, 29]. However, the most important one is the discreteness of the underlying space. Consider for example, the Frenkel-Kontorova (FK) model. It is the spatially discretizd s-G equation. While the s-G equation which is the long wavelength approximation of the FK model is integrable, the FK model in its generic form is nonintegrable. This nonintegrablity arises from the discretization reflecting the discreteness of the space[30]. The other interesting as well as important example, of course is the already mentioned DNLSE[9, 10, 11]. So, relevant in this context is the study of an IN-DNLS, and also the modified Salerno equation (MSE)[21, 31]. The IN-DNLS is a hybrid form of the ALDNLSE and the DNLSE with a "tunable" nonlinearity. On the other hand, in the MSE, the usual DNLSE is replaced by a modified version of the DNLSE, the ADNLSE which involves acousitc phonons, instead of optical phonons in condensed matter physics parlance[22]. These equations are studied with the prime objective to understand the role of lattice discreteness as a mechanism for the collapse of moving self-localized states to stable, but pinned localized states[21, 31]. We further note that an IN-DNLS, which can be continually switched from the DNLSE to the ALDNLSE by varying a single parameter, is also studied to investigate the discreteness induced oscillatory instabilities of dark solitons[32].

There is at least one continuous nonlinear equation, "ϕ^4 equation", which is nonintegrable, contrary to its "cousin" s-G system. This ϕ^4 equation can have either solitary wave solutions or "kink-like" solutions with permanent profile. However, these solutions do not have the simple collision properties of solitons. These solutions can bump, lock or annihilate each other. In addition these always emit some oscillatory disturbances or radiation in the course of a collision. Furthermore, the head-on collisions of kink and antikink pair of solutions of ϕ^4 equation will settle either to a bound state (bion) or to a two-soliton solution. This settling down is found to depend fractally on the impact velocity. We further note that all solutions ϕ^4 equation have profound physical as well as theoretical significance[33, 34, 35, 36, 37]. In continuation, we mention that the appearance of fractal structure in the kink-breather interaction is investigated using the FK model[30]. Similarly, a fractal structure in solitary-wave collisions for the coupled NLS equations is reported. This structure is observed in the separation velocity versus collision velocity graph[38].

On the contary, to the best of my knowledge there is no known analogy of ϕ^4 type of equation in the discrete case. Here I propose an extended nonintegrable version of the ALDNLSE, which has a "tunable" nonlinearity in the intersite hopping term. At the same time, the form of nonlinearity is such that it can allow solitary wave like solutions, as seen in ϕ^4 equation, and its suitable parallel in the linear regime is one-dimensional correlated disordered systems[39, 40]. Inasmuch as this nonlinearity is in the intersite hopping term, it serves two important purposes. First of all, this extra dispersive correction to the ALDNLSE will try to destroy the Ablowitz-Ladik (A-L) soliton by dispersion. So, by varying this term we can investigate the effect of dispersive imbalance on the maintance of the moving solitonic profile. It is relevant at this point to note that both the IN-DNLS and the MSE investigate the competition between the on-site trapping and the solitonic motion of the A-L solitons. In case of the MSE, it is found that the narrow A-L solitons, having width smaller than the critical width will get pinned by the lattice potential[21, 22]. Similar results are obtained numerically from the IN-DNLS[31]. Secondly, since the extra dispersive term in the proposed equation breaks the integrability of the ALDNLSE, the dynamics of the A-L solitons will not be transparent to the lattice discreteness. So, along with the IN-DNLS and the MSE, this model also gives an opportunity to study further the effect of Peierls-Nabarro (PN) potential on the dynamics of solitons[31, 41]. We further note that the DHM yields a very complicated nonlinear discrete differential equation[21]. So, to gain a better understanding of the DHM, a somewhat simpler but physically relevant system needs to be considered[21]. This is another important motivation of this study. It is in fact noteworthy in this context that a slightly modified ALDNLSE has been studied as a plausible model for dynamical self-trapping in discrete lattices[42]. As for further motivation of this study, we note that one rapidly emerging field in nonlinear dynamics is the study of the solitary-wave interaction in nonintegrable nonlinear models. The emergence of this field is due to the possibility of observing many of the predicted effects experimentally, including the soliton energy and momentum exchange[30, 33, 34, 35, 36, 37, 38, 43, 44]. The model, that is to be proposed here allows with an opportunity to study the head-on collision of scalar lattice solitary waves. Finally, nonlinear phenomena are quite a common occurence in all branches of natural science. But, our theoretical understanding of nonlinear equations, particularly that of nonlinear discrete differential equations is quite limited. So, when viewed from this angle, another important dimension gets added to the present study.

The organisation of the paper is as follows. In what follows, I first propose a set of discrete nonintegrable Hamil-

tonians, and derive the equation of interest from the requisite Hamiltonian. I study then analytically the existence of moving solitary wave like solution in this equation. Since this equation is a perturbated Ablowitz-Ladik equation, I study this problem further using a standard perturbative method to find trapped and moving solitons. I consider next the formation of stationary localized states and the effective masses of these states. Subsequently, I present some numerical results to substantiate the analysis. I also study the collison of two solitary wave profiles numerically using the equation. Findings from my study are summarized at the end . In this section I also discuss the applicabilty and future scopes of the present work.

II. A GENERAL DERIVATION OF THE ABLOWITZ-LADIK CLASS OF NONLINEAR EQUATIONS

We consider here the following Hamiltonian, H.

$$\begin{aligned} \mathrm{H} &= J \sum_n (\phi_n^\star \ \phi_{n+1} \ + \ \phi_{n+1}^\star \ \phi_n) \ - \ \frac{1}{2} \sum_n \ \sum_{j \ = \ 1}^{l} g_0^j \ (\phi_n^\star \ \phi_{n+j} \ + \ \phi_{n+j}^\star \ \phi_n)^2 \ + \frac{2\nu}{\lambda} \ \sum_n |\phi_n|^2 \\ &- \ \frac{2}{\lambda} \ (\frac{\nu}{\lambda} \ - \ J) \ \sum_n \ln [1 \ + \ \lambda \ |\phi_n|^2]. \end{aligned} \tag{2.1}$$

It is understood that the Hamiltonian, H in Eq.(2.1) describes a conservative system in which a quasiparticle (exciton, vibron etc.) moves in an one-dimensional chain. To obtain the time evolution equations for generalized coordinates, $\{\phi_m, \ \phi_m^\star\}$, we make use of the nonstandard Poisson bracket relationship among these generalized coordinates as given in Appendix A. After defining $\phi_m \ = \ (-1)^m \ \psi_m$, we get for $m \ = \ 1, 2, \ \ldots$

$$\begin{aligned} \mathcal{F}_j(\psi_m, g_0^j) &= g_0^j \sum_{\sigma \ = \ \pm 1} (\psi_m^\star \ \psi_{m+\sigma j} \ + \ \psi_{m+\sigma j}^\star \ \psi_m) \ \psi_{m+\sigma j} \\ \mathcal{F}(\psi_m, \lambda) &= (1 \ + \ \lambda \ |\psi_m|^2) \ \sum_{j \ = \ 1}^{l} \mathcal{F}_j(\psi_m, g_0^j) \end{aligned} \tag{2.2}$$

$$i \ \dot{\psi}_m - \ 2J \ \ \psi_m \ + \ J \ (1 \ + \ \lambda \ |\psi_m|^2) \ (\psi_{m+1} \ + \ \psi_{m-1}) \ = \ 2 \ \nu \ |\psi_m|^2 \ \psi_m \ - \ \mathcal{F}(\psi_m, \lambda). \tag{2.3}$$

In $\mathcal{F}(\psi_m, \lambda)$, arguements, $g_j^0, \ j \ = \ 1, 2, \cdots, \ l$ have been suppressed, and $J \ > \ 0$. When $l \ = \ 1$, in Eq.(2.1) and consequently in Eq.(2.3) we have just an extra nonlinear nearest-neighbor coupling in hopping with a coupling constant, g_0^1. This coupling is assumed to arise due to quasiparticle-phonon interaction[21]. Similarly, when $l \ = \ 2$, we have both nonlinear nearest-neighbor and next-nearest-neighbor couplings. Coupling constants are g_0^1 and g_0^2 respectively. So, in this model coupling constants are assumed to depend on the distance between the sites involved. For any arbitrary l then, a given site, over and above the standard linear nearest-neighbor coupling, is coupled through nonlinear hopping to l consecutive sites in general on both sides of it. Of course, the origin of such coupling is assumed to arise due to the heuristic generalization of quasiparticle-phonon interaction beyond the nearest neighbor. We further note that in this model also

$$\mathcal{N} = \sum_{m = \ -\infty}^{\infty} \ln [1 + \ \lambda \ \ |\psi_m|^2] \ = \ \text{Constant} \tag{2.4}$$

as in the original Ablowitz -Ladik equation (see also appendix A). So, if $\lambda \ |\psi_m|^2 \ \ll \ 1$ for all m, we get $\sum_m |\psi_m|^2 \ \approx$ Constant. We now consider the following limits of Eq.(2.3). (1) When $g_0^j \ = \ 0$ for all j, we have the Salerno Equation in the quantum version. In the classical domain, it has been nomenclatured as IN-DNLS and the formation of staggered localized states from this equation is studied[31, 45, 46]. (2) When $\nu \ = \ 0$ as well $g_0^j \ = \ 0$ for all j, we have the standard Ablowitz-Ladik equation. This equation is known to have a single soliton solution[6, 7]. (3) When $\lambda \ = \ 0 \ = \ \nu$ and also $l \ = \ 1$, we have the model where exciton-phonon interaction affects only the hopping between nearest-

neighbors. Of course, to obtain this particular nonlinear mathematical form of interaction, it is assumed that the lattice relaxation is faster than the quasiparticle dynamics[21]. This is a very standard assumption which is used in the Davydov's soliton[13, 22] and also in the Rashba and Toyozawa mechanism for the formation of self-trapped exciton[47, 48, 49]. This equation is also studied for single soliton solution, using perturbation method[21]. (4) The equation with $\nu = 0$ will be refered to here as the nonintegrable Ablowitz-Ladik (N-AL) equation. Consider again the situation where we take $l = 1$ in the N-AL equation and further ignore altogether in Eq.(2.3) the term having $g_0^1\ \lambda$. We have then a model equation which describes a truncated version of the model, in which exciton(vibron)-phonon interaction affects both site-energy and hopping. We note that a perturbative analysis of the full model is done for one soliton solution[21]. Here our plan is to analyze various aspects of the N-AL equation.

Before we proceed furthere, we define $\tau = Jt,\ \Psi_m = \sqrt{\lambda}\ \psi_m,\ m \in Z$, and $g_j = \frac{g_0^j}{\lambda\ J}$. We further note that $\mathcal{F}_j(\frac{\Psi_m}{\sqrt{\lambda}}, g_0^j) = \frac{1}{\sqrt{\lambda}}\ \mathcal{F}_j(\Psi_m, g_j),\ j = 1, 2, \cdots l$. This, in turn yields $\mathcal{F}(\frac{\Psi_m}{\sqrt{\lambda}},\ \lambda) = \frac{1}{\sqrt{\lambda}}\ \mathcal{F}(\Psi_m, 1),\ m \in Z$. So, in the limit of $\nu = 0$, we have from Eq.(2.3) and $m \in Z$

$$i\ \dot{\Psi}_m\ -\ 2\ \Psi_m\ +\ (1\ +\ |\Psi_m|^2)\ (\Psi_{m+1}\ +\ \Psi_{m-1}) = -\ \mathcal{F}(\Psi_m, 1) \qquad (2.5)$$

and Eq.(2.4) also remains valid with $\lambda = 1$ and ψ_m replaced by Ψ_m. Again, $\mathcal{F}(\Psi_m, 1)$ should have in its arguement $g_1,\ g_2, \cdots,\ g_l$, which have been suppressed for convenience. We note that Eq.(2.5) possesses a reflection symmetry. To understand this, we consider the transformation, $\Psi_m \rightarrow (-1)^m\ \Psi_m\ \exp[-4i\tau]$. The equation will remain invariant under this transformation provided $\tau \rightarrow -\tau$ and $g_j \rightarrow -g_j,\ \ j \in l$. Again, if $\mathcal{F}(\Psi_m, 1) = 0,\ m \in Z$, the equation becomes self-dual under this reflection transformation.

III. PROPAGATING SOLUTIONS OF EQ.(2.5)

In order to gain an understanding of the nature of the solution of Eq.(2.5), we consider the case where $g_j = 0$ for all j. As mentioned earlier, in this limit we have the integrable Ablowitz-Ladik discrete nonlinear Schrödinger equation(ALDNLSE)[6, 7]. The exact one-soliton solution of the ALDNLSE, $\Psi_m^0,\ m \in Z$ is

$$\begin{aligned}\Psi_m^0(\tau) &= \frac{\sinh\mu}{\cosh[\mu(m-x)]}\exp[ik(m-x) - i\alpha] \\ &= Q_m(\tau)\ \exp[ik(m-x) - i\alpha] \qquad (3.1)\end{aligned}$$

with the following equations for the soliton parameters:

$$\dot{\mu} = 0,\ \dot{k} = 0,\ \dot{\alpha} = \omega, \qquad (3.2)$$

$$\omega = 2\ [1 - \cosh\mu\cos k], \qquad (3.3)$$

$$\dot{x} = \frac{2}{\mu}\sinh\mu\ \sin k. \qquad (3.4)$$

So, for each μ there exists a band of velocities [see Eq.(3.4)] at which the localized state or the one-soliton state can travel without experiencing any PN pinning due to the lattice discreteness[31, 41]. We also note that for a given $k,\ \mu \in [0, \infty]$. Mathematically, one soliton solution of the ALDNLSE describes two parameters, namely k and μ, family of curves. So, even if we pin the value of one of those parameters to a prescribed value, Eq.(3.1) will still be a solution of the ALDNLSE.

We now consider $\mathcal{F}(\Psi_m^0, 1)$. Introducing Eq.(3.1) in Eq.(2.5) we get

$$\frac{\mathcal{F}(\Psi_m^0, 1)}{2\ (1 + Q_m^2)\ \Psi_m^0(\tau)} = \sum_{j\ =\ 1}^{l}\{g_j\ \cos kj\ [(Q_{m+j}^2\ +\ Q_{m-j}^2)\ \cos kj\ \ +\ i(Q_{m+j}^2\ -\ Q_{m-j}^2)\ \sin kj]\}. \qquad (3.5)$$

For convenience in further discussion, we consider only one term, say the l-th term of the sum in Eq.(3.5). We note that for $\cos kl = 0$, permissible values of k are $k = \pi - (\frac{2j_1+1}{l})\ (\frac{\pi}{2}),\ \ j_1 = 0, 1, 2, \cdots, (2l-1)$. So, there are $2l$ permissible values of k for $k \in [-\pi, \pi]$. We now state the following results.

(1) For $l = 1, \mathcal{F}(\Psi_m^0, 1) = 0$ for $m \in Z$, if $|k| = \frac{\pi}{2}$. So, for this case Eq.(3.1) with $k = \pm\frac{\pi}{2}$ are the solitary wave like solutions of Eq.(2.5). We further note that solitary waves have the maximum possible speed.

(2) l is odd as well only odd values of j in the sum in the Hamiltonian, H are permissible. Also,in this case, only $|k| = \frac{\pi}{2}$ is allowed. So, Eq.(3.1) with these particular values of k are the solitary wave like solutions of Eq.(2.5).

(3) l is even as well only even values of j in the sum in Eq.(3.5) are permissible. In this case, there is no permissible value of k. So, Eq.(2.5) will not have any solitary wave like solution.

(4) l is arbitrary and j takes odd values with at least one even value. In this case, even if l is odd, there is no permissible value of k. So, Eq.(2.5) has no solitary wave like solution.

(5) There is only one term, say l-th term in the sum in Eq.(3.5). In this situation, Eq.(3.1) describes the solitary

wave like solution of Eq.(2.5) with $2l$ permissible values of k which are already given.

We also note that when $|g_j| << 1$ for $j = 1, 2, \cdots l$, Eq.(2.5) then can be treated as a perturbed ALDNLSE. In this situation we can use the standard perturbation theory to investigate the soliton dynamics from Eq.(2.5). This aspect is considered next.

IV. THE PERTURBATIVE SOLITON DYNAMICS OF EQ.(2.5)

The method is amply discussed in the literature[21, 22, 50]. In this method, it is assumed that the zeroth order solution is the standard one-soliton solution of the ALDNLSE. It is further assumed that the effect of perturbation on the soliton dynamics can be adequately taken into consideration by allowing four parameters, namely x, k, μ and α to vary adiabatically in time, τ. Application of the method to the N-AL equation gives for μ, k and x :

$$\begin{aligned} S(\mu,x) &= \sum_{s\,=\,1}^{\infty} \frac{\frac{\pi^2 s}{\mu}}{\sinh\frac{\pi^2 s}{\mu}}\,\cos 2\pi s x \\ G(k,l,\mu) &= \sum_{j\,=\,1}^{l} g_j\,\frac{\cos^2 kj}{\sinh^2\mu j} \\ G_1(k,l,\mu) &= 4\,\frac{\sinh^4\mu}{\mu^2}\,[\mu\,\coth\mu\,-\,1-2\,S(\mu,x)] \\ G_2(k,l,\mu) &= G_1(k,l.\mu)\,\frac{\partial G(l,k,\mu)}{\partial k} \end{aligned}$$

$$\dot{\mu} = 0 \tag{4.1}$$

$$\dot{k} = -\;8\;\frac{\sinh^4\mu}{\mu^2}\,G(k,l,\mu)\,\frac{\partial S(\mu,x)}{\partial x} \tag{4.2}$$

$$\dot{x} = -\;2\;\frac{\sinh\mu}{\mu}\,\frac{\partial\cos k}{\partial k}\;-\;G_2(k,l,\mu). \tag{4.3}$$

We first note thar the famous Poisson sum formula is used to obtain $S(\mu,x)$ and $G(k,l,\mu)$[21]. In the situation where $\cos kj = 0$ for all j, both $G(k,l,\mu)$ and $\frac{\partial G(l,k,\mu)}{\partial k}$ are zero. In this case, it is easy to see that $\dot{\mu}$, $\dot{k}$ and $\dot{x}$ are given by Eq.(3.2) and Eq.(3.4) respectively. Of course, for $\dot{x}$ only certain values of k for $k \in [-\pi, \pi]$ are allowed. Notwithstanding this, this case is as expectedly similar to the one-soliton solution of the ALDNLSE. We consider next the problem of an effective Hamiltonian.

A. An effective Hamiltonian

In order to derive an effective Hamiltonian for the dynamical system described by Eqs.(4.2) and (4.3), we mutiply these two equations by $\dot{x}$ and $\dot{k}$ respectively. Now, substracting the first one from the second one, we get

$$-[2\,\frac{\sinh\mu}{\mu}\,\frac{\partial\cos k}{\partial k}+4\,\frac{\sinh^4\mu}{\mu^2}\,[\mu\,\coth\mu-1-2\,S(\mu,x)]\,\frac{\partial G(l,k,\mu)}{\partial k}]\,\dot{k}+8\,\frac{\sinh^4\mu}{\mu^2}\,G(k,l,\mu)\,\frac{\partial S(\mu,x)}{\partial x}\,\dot{x}\;=\;0. \tag{4.4}$$

It is easy to see that Eq.(4.4) defines a constant of motion of the dynamical system. This constant can be called the effective Hamiltonian, $H_{\rm eff}(x,k,\mu,l)$ of the system and from Eq.(4.4) we get

$$H_{\rm eff}(x,k,\mu,l) \;=\; -2\,\frac{\sinh\mu}{\mu}\;\cos k\;-\;4\,\frac{\sinh^4\mu}{\mu^2}\,[\mu\;\coth\mu\;-\;1-2\,S(\mu,x)]\,G(l,k,\mu). \tag{4.5}$$

Again, it is easy to see from Eq.(4.4) that

$$\dot{x} \;=\; \frac{\partial H_{\rm eff}}{\partial k}\quad\text{and}\quad \dot{k} \;=\; -\,\frac{\partial H_{\rm eff}}{\partial x} \tag{4.6}$$

together yield the original equations of $\dot{x}$ and $\dot{k}$. In the subsequent analysis, the $l = 1$ case being the physically most relevant one, is analyzed. In another simplification, $S(\mu,x)$ is approximated by its the most dominant first term. This simplification will not bring any qualitative change in the dynamics.

B. The analysis of fixed point

To obtain the fixed points of the set of equations, namely Eq.(4.2) and Eq.(4.3), we set $\dot{x_s} = 0 = \dot{k_s}$. This then gives $(x_s, k_s) = (\frac{p}{2}, n\pi)$ where p and $n = 0,\ \pm1,\ \pm2,\ \cdots$. To find the phase portraits around these

fixed points, we define $z_1 = x - x_s$ and $z_2 = k - k_s$. We define for convenience and clarity

$$\begin{aligned} A_0(\mu) &= \frac{\sinh\mu}{\mu} \\ A_1(\mu) &= A_0^2(\mu)\ (\mu\ \coth\mu\ -1) \\ A_2(\mu) &= A_0^2(\mu)\ \frac{\frac{\pi^2}{\mu}}{\sinh\frac{\pi^2}{\mu}}. \end{aligned} \tag{4.7}$$

We further define

$$\begin{aligned} B_0(\mu,p) &= A_1(\mu)\ -\ (-1)^p\ 2\ A_2(\mu) \\ B_1(\mu,g_1,p,n) &= (-1)^n A_0(\mu)\ +\ 4\ g_1\ B_0(\mu,p) \\ B_2(\mu,g_1) &= 16\ \pi^2\ g_1\ A_2(\mu). \end{aligned} \tag{4.8}$$

Now, because of our stated assumptions, we get

$$\begin{aligned} \dot{z_1} &= 2\ B_1(\mu,g_1,p,n)\ z_2 \\ \dot{z_2} &= (-1)^p\ 2\ B_2(\mu,g_1)\ z_1. \end{aligned} \tag{4.9}$$

This set of equations, in turn yields

$$\frac{z_1^2}{B_1(\mu,g_1,p,n)}\ -\ (-1)^p\ \frac{z_2^2}{B_2(\mu,g_1)}\ =\ \text{Constant.} \tag{4.10}$$

From Eq.(4.10), it is transparent that the system has only two types of fixed points. These are centres and saddle hyperbolic fixed points. We give below some in depth analysis of fixed points.

We note that $A_i(\mu),\ i = 0,1,2$ are even fuctions of μ. This, in turn implies that $B_i,\ i = 0,1,2$ are also even functions of μ. We take $g_1 > 0$ in this analysis. There will be no loss of generality by this assumption. We now note the followings.

(i) $B_0(\mu,p) \to 0$, as $\mu \to 0$. It can also be shown that $B_0(\mu,p)$ is a monotonically increasing function of μ. In other words, it is a monotonically increasing positive semidefinite function of μ. These properties are true, irrespective of p being even or odd.

(ii) $B_1(\mu,g_1,p,n) \to (-1)^n$, as $\mu \to 0$. Furthermore, it can be seen by plotting this function against μ that $B_1(\mu,g_1,p,n) > 0$, when $\mu \to \infty$. Both properties are true irrespective of the nature of p. Furthermore, when n is even, $B_1(\mu,g_1,p,n)$ is a monotonically increasing as well as a positive definite function of μ. On the other hand, when n is odd, there exists a value of μ, say $\mu_r(g_1,p)$ such that $B_1(\mu_r,g_1,p,n) = 0$. Again, $\mu_r(g_1,p)$ has the following properties. (a) For a given value of g_1, $\mu_r(g_1,\ evenp) > \mu_r(g_1,\ oddp)$, (b) irrespective of the nature of p, the value of μ_r monotonically decreases with increasing g_1, and (c) $\mu_r(g_1,\ evenp) \to \mu_r(g_1,\ oddp)$ as $g_1 \to \infty$. See also Fig.1.

(iii) $B_2(\mu,g_1)$ is a monotonically increasing positive semidefinite function of μ.

We now consider case by case to determine the nature of fixed points from the linearized analysis. We note that the classifications are done using standard analysis[51, 52].

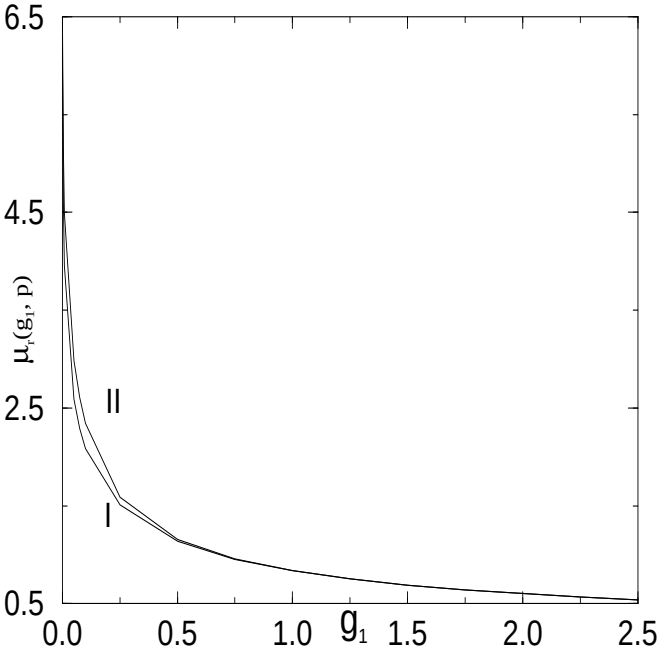

FIG. 1: This shows the variation of $\mu_r(g_1,p)$ as a function of g_1 where μ_r is the root of $B_1(\mu,g_1,p,n)$. Eq.(4.8) in the text. n is odd. I: p is odd and II: p is even.

Case I : n and p are both even. In this case, both $B_1(\mu,g_1,p,n)$ and $B_2(\mu,g_1)$ are positive. Eq.(4.10) defines a hyperbola. So, the fixed point is a saddle point.

CaseII ; n is even, but p is odd. Since, the nature of these two functions remains the same, Eq.(4.10) defines an ellipse. So, we have a center.

Case III: Both n and p are odd. Again, $\mu > \mu_r(g_1,evenp)$. In this case, both B_1 and B_2 are positive. So, Eq.(4.10) defines an ellipse and we have a center.

Case IV: n is odd, but p is even. Furthermore, $\mu > \mu_r(g_1,evenp)$. In this case also, both B_1 and B_2 are positive. But due to the evenness of p, Eq.(4.10) defines a hyperbola and we have a saddle point.

Case V: Both n and p are odd, but $\mu < \mu_r(g_1,oddp)$. In this case, while B_2 is positive, B_1 is negative. So, Eq.(4.10) defines a hyperbola and the fixed point is a saddle point.

Case VI: n is odd, but p is even. Again, $\mu < \mu_r(g_1,oddp)$. In this case, Eq.(4.10) defines an ellipse. So, we have a center.

Case VII: Both n and p are odd. Again, $\mu_r(g_1,oddp) < \mu < \mu_r(g_1,evenp)$. In this case, both B_1 and B_2 are positive. Since, p is odd, Eq.(4.10) defines an ellipse. So, we have a center.

Case VIII: n is odd, but p is even. Furthermore, $\mu_r(g_1,oddp) < \mu < \mu_r(g_1,evenp)$. In this case, while B_1 is negative, B_2 is, however, positive. Since, p is even, Eq.(4.10) defines an ellipse. So, we have a center.

Our analysis is tabulated below. By Region I, it is meant

that $\mu < \mu_r(g_1, oddp)$. Region II and III are respectively characterized by $\mu_r(g_1, oddp) < \mu < \mu_r(g_1, evenp)$ and $\mu > \mu_r(g_1, evenp)$.

TABLE I : Nature of fixed points from linearization analysis

$x_s = \frac{p}{2}$	$k_s = n\,\pi$	Nature of fixed points		
p	n	Region I	Region II	Region III
even	even	saddle	saddle	saddle
odd	even	center	center	center
odd	odd	saddle	center	center
even	odd	center	center	saddle

C. A numerical analysis of phase portraits

Regarding the numerical investigation of phase diagrams around fixed points, we note that there are all together six fundamental possibilities. Two possibilities arise from k_s being even or odd. Again, for each case, there are three possibilities, depending on the magnitude of μ. In this discussion, we consider $k_s = 0$ and π. Along the line, $k_s = 0$, we have a set of fixed points at $x_s = 0, \pm\frac{1}{2}, \pm1, \pm\frac{3}{2}, \pm2, \cdots$. According to the analysis, based on linearization $x_s = 0, \pm1, \pm2, \cdots$ should be saddle hyperbolic fixed points. Between every two consecutive saddle points, one should naturally expect centers. This is perfectly borne out in the numerical investigation (Fig.2). It is also to be noted that Fig.2 shows the phase diagram in the region I ($\mu < \mu_r(g_1, oddp)$). To understand the origin of a saddle fixed point between two consecutive centers, we note that two outermost ellipses encircling two centers will definitely touch at a point on the x-axis. Then, the flow of phase curves emanating from this point as well as in the vicinity of it will indicate a saddle hyperbolic fixed point. By the similar type of argument, the appearance of a center between two consecutive saddle fixed points can be understood. It is also found that the absolute critical value of k, below which localization of soliton occurs, increases monotonically with increasing μ. This behavior is consistent with the physics of the problem.

We consider now the case of $k_s = \pi$. It has certain interesting twists, which is quite a common occurence in the dynamics of nonlinear systems[52]. In the region I, that is, $\mu < \mu_r(g_1, oddp)$, according to our standard linearization based analysis, $x_s = 0, \pm1, \pm2, \cdots$ should be centers. On the other hand, $x_s = \pm\frac{1}{2}, \pm\frac{3}{2}, \cdots$ should be saddle hyperbolic fixed points. The reason to have a saddle hyperbolic fixed point between two consecutive centers has already been put forward in the previous paragraph. Our numerical investigation also confirms this result (Fig.2). In the region II ($\mu_r(g_1, oddp) < \mu < \mu_r(g_1, evenp)$), the linearization analysis tells us that all fixed points along the line $k_s = \pi$ are centers. To understand this scenario, we note the following. Consider two centers, which are next but one to each other. Outermost ellipses, encircling these fixed points can also intersect. We then have a convex lens type region in the phase space (Fig.3). Within this region of phase space,

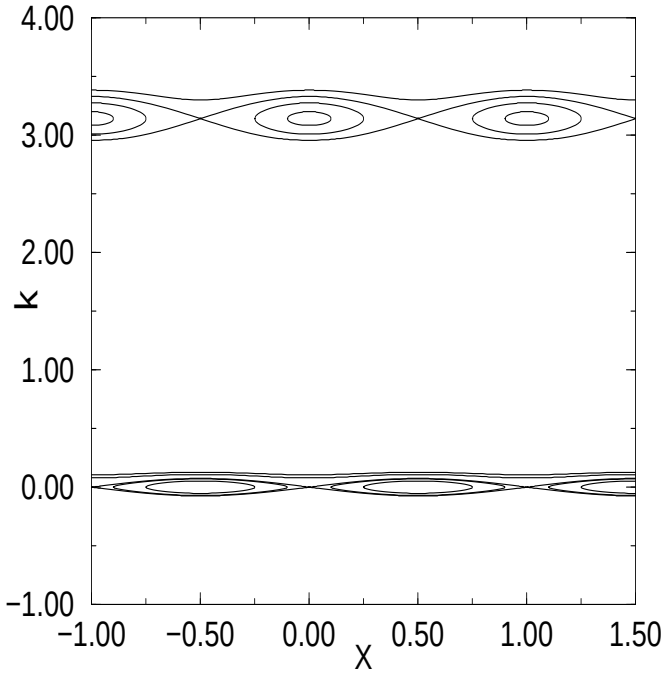

FIG. 2: The bottom part of the figure is the phase portrait that shows the trapped and the moving solitons in Region I for the fixed points having $k_s = 0.0$. For moving solitons $k_{m0} = \frac{\pi}{40}$ and $\frac{\pi}{30}$ respectively. The upper part of the figure is the phase portrait that shows the trapped and the moving solitons in Region I, but for the fixed points having $k_s = \pi$. For the moving soliton $k_{m\pi} = \frac{21\pi}{20}$. $\{x_s\}$ are shown in the figure. $l = 1, g_1 = 0.5$, and $\mu = 1.0$ for all curves in the figure. Eq.(4.5) is used to obtain this phase portrait. See also the text.

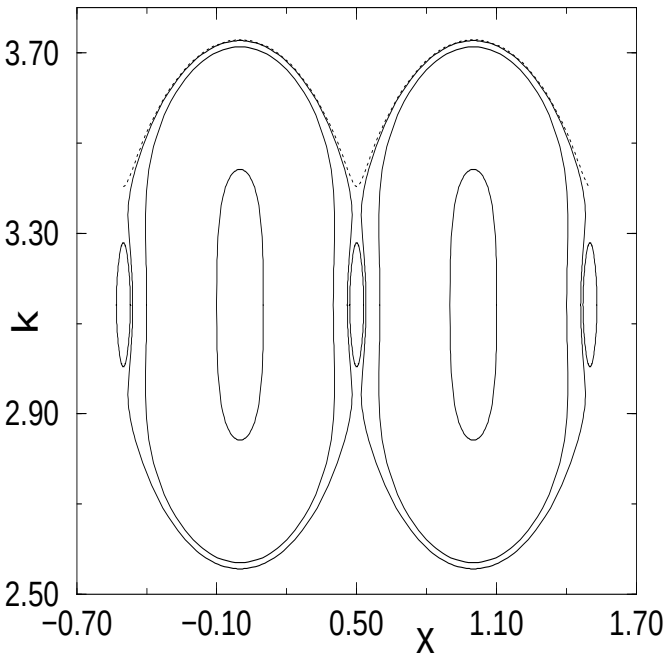

FIG. 3: This phase portrait shows the trapped and the moving solitons in Region II for fixed points having $k_s = \pi$. $\{x_s\}$ are, of course, shown in the figure. As per the text $l = 1$. Other parameters, namely $g_1 = 0.5$, and $\mu = 1.15$. For the moving soliton $k_{m\pi} = \frac{13\pi}{}$

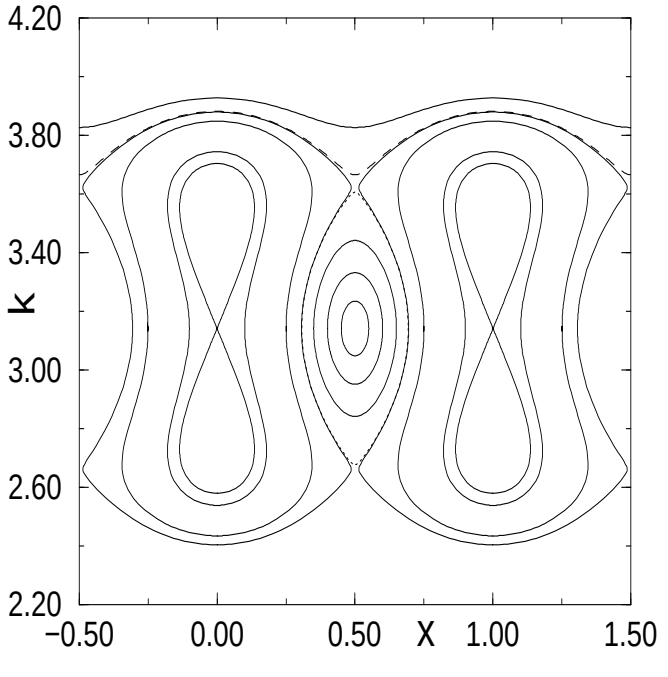

FIG. 4: This phase portrait shows the trapped as well as the moving solitons in Region III for fixed points having $k_s = \pi$. $\{x_s\}$ are, of course, shown in the figure. As per the text $l = 1$. Furthermore, $g_1 = 0.5$, and $\mu = 1.2$. For the moving soliton $k_{m\pi} = \frac{7\pi}{6}$ and $\frac{5\pi}{4}$.

phase curves will have no other option but to close around a point on the x-axis. This fixed point will also then be another center. This is clearly seen in Fig.3, which describes the phase diagram of the soliton dynamics in the region II.

It is needless to say that the phase diagram is very interesting and unique. To the best of my knowledge, this is the first case where a chain of centers with no hyperbolic fixed point is found. The phase diagram in the region III is shown in Fig.4.

This region is defined by $\mu > \mu_r(g_1, evenp)$. According to the linearization analysis, along the line $k_s = \pi$, $x_s = \pm\frac{1}{2}, \pm\frac{3}{2}, \cdots$ should be centers. This is indeed found in the numerical investigation. Again, the same linearization analysis tells that $x_s = 0, \pm1, \pm2, \cdots$ will be saddle hyperbolic fixed points. From the numerical study with $\mu = 1.2$ and $g_1 = 0.5$, we find that upto a certain distance from each of these fixed points, phase curves tend to diverge from the fixed points, indicating their hyperbolic structure. However, after a critical value of x, phase curves turn back to make close curves. This happens upto a certain maximum value of x from the relevant fixed point on the line $k_s = \pi$. After that value of x, phase curves close around the nearest center (Fig.4). In case of $x_s = 0$, it is found that the phase curve with the intial value of x, $x_0 = 0.306$ closes around

$x_s = 0$. But, for $x_0 = 0.307$, the phase curve encircles $x_s = 0.5$. So, for these two fixed points, the transition point is somewhere in between these two values.

It is important to realize that in this part of the problem we find three important phenomena that are encountered in nonlinear dynamics, namely (i) bifurcation, (ii) discrete breathers and (iii) relaxation oscillations[51, 52, 53, 54]. We note that for $\mu > \mu_r(g_1, oddp)$, that is, in regions II and III, all saddle points are changed to centers (Fig.3 and Fig.4). So, we obtain a bifurcation in the phase portrait at $\mu = \mu_r(g_1, oddp)$. Furthermore it is a saddle-center bifurcation. Again, at this bifurcation point, it is easy to show that we have spatially localized but time periodic solutions. These localized solutions can be pinned at one of the permissible values of x_s, namely at $x_s = \pm\frac{1}{2}, \pm\frac{3}{2}, \cdots$. These are by definition discrete breathers[54]. To see it further, we examine Eq.(4.9). Since at $\mu = \mu(g_1, oddp)$, $B_1 = 0$, from the first equation of Eq.(4.9) we find that $\dot{z_1} = 0$. The consistent solution is then $z_1 = 0$. This in turn gives $x = x_s(oddp) = (l_1 + \frac{1}{2})$ where $l_1 = 0, \pm1, \pm2 \cdots$. Then the second equation of Eq.(4.9) gives $\dot{z_2} = 0$. This implies that $k = k_s = (2l_2 + 1)\,\pi$ where $l_2 = 0, \pm1, \pm2, \cdots$. For this particular case , $k_s = \pi$ or $l_2 = 0$. From the perturbative calculation of α appearing in Eq.(3.1)[22], it can be easily shown that α is proportional to $\tau = Jt$. The energy of the breather in terms original variables[31] is

$$\begin{aligned}
\tilde{E}[\mu_r(g_1, oddp)] &= 1 + 2g_1\,\frac{\sinh\mu_r(g_1, oddp)}{\mu_r(g_1, oddp)}\,[1 - \mu_r(g_1, oddp)\,\coth\mu_r(g_1, oddp) + \sum_{s=1}^{\infty}(-1)^s\,\frac{\frac{\pi^2 s}{\mu_r(g_1, oddp)}}{\sinh\frac{\pi^2 s}{\mu_r(g_1, oddp)}}] \\
E_{breather} &= H[\mu_r(g_1, oddp)] = \frac{4J}{\lambda}\sinh\mu_r(g_1, oddp)\;\tilde{E}[\mu_r(g_1, oddp)]. \qquad (4.11)
\end{aligned}$$

We also note that for $\frac{J}{\lambda} > 0$, this is the minimum energy spatially localized state. Inasmuch as Eq.(2.5) has a reflection symmetry, another discrete breather will be obtained by the transformation, $g_1 \to -g_1$. This is discussed later. We again note that our linearization analysis suggests that at $\mu = \mu(g_1, evenp)$, we have another bifurcation. This time it is a center saddle bifurcation. However, we find that in the region III the phase portraits around $x_s = 0, \pm1, \pm2 \cdots$ are not that of saddle points. In stead these phase diagrams consisting of closed orbits, are made up of both stable and unstable manifolds[52]. So, here we have a relaxation oscillations dynamics as seen in Van der Pol oscillators[51, 55], in the Zeeman models of heartbeat and nerve impulse[56]. We further note that in the present problem any relaxation oscillations dynamics is not physically allowed. So, these parts of the phase space will remain unaccessible to the system.

V. STATIONARY LOCALIZED STATES

To study stationary localized states of Eq.(2.5), we seek for an oscillatory solution in the form[31]

$$\Psi_m(\tau) = Q_m(\tau)\,\exp[i(km - \omega\tau + \sigma_0)]\,\exp[-2i\tau]\,, \qquad m \in Z \qquad (5.1)$$

where Q_m is real and σ_0 is a constant phase factor. From the real and imaginary parts of Eq.(2.5), we have

$$\begin{aligned}
(\hat{\Omega}\hat{Q})_m &= \omega\,Q_m + \cos k\,(1 + Q_m^2)\,(Q_{m+1} + Q_{m-1}) \\
&+ 2\,(1 + Q_m^2)\,Q_m \sum_{j=1}^{l} g_j \cos^2 kj\,(Q_{m+j}^2 + Q_{m-j}^2) = 0; \qquad (5.2) \\
\dot{Q}_m &+ \sin k\,(1 + Q_m^2)\,(Q_{m+1} - Q_{m-1}) \\
&= -2\,(1 + Q_m^2)\,Q_m \sum_{j=1}^{l} g_j \cos kj\,\sin kj\,(Q_{m+j}^2 - Q_{m-j}^2) \qquad (5.3)
\end{aligned}$$

where $\hat{Q}$ is the column vector $(Q_1, Q_2, \cdots\ Q_m\ \cdots)$ and $\hat{\Omega}$ is the matrix defined by the left hand side of

Eq.(5.2). Eq.(5.2) with vanishing boundary condition constitutes a nonlinear eigenvalue problem for localized states[10, 11, 31]. Eq.(5.3) determines the time evolution of the localized states. It is a trite algebra to show that when $g_j = 0$ for all j, $Q_m(\tau)$ given by Eq.(3.1) is a solution of Eq.(5.2) and Eq.(5.3). When $k = 0$ or π, Q_m, $m \in Z$ is stationary. A localized state is called "staggered" if $k = \pi$, and "unstaggered" if $k = 0$. We further observe that under the transformation, $Q_m \rightarrow (-1)^m Q_m$, Eq.(5.2) will remain invariant if $\omega \rightarrow -\omega$ and $g_j \rightarrow -g_j$ $j \in l$. This is indeed in accordance with the reflection symmetry of Eq.(2.5). This result in turn implies that if an unstaggered localized state, $Q_m \exp[-i\omega\tau]$ is a solution of Eq.(5.2), the corresponding staggered localized state, $(-1)^m Q_m \exp[i\omega\tau]$ is then a solution of the same, provided g_j, $j \in l$ changes sign for all j. To determine locations of these localized states, we shall specialize on $l = 1$ case. This simplification will not affect the merit of the discussion. From Eq.(5.2), we have

$$\omega = -2\cos k - (\cos k + 2g_1 \cos^2 k) \frac{\sum_m Q_m^2 (Q_{m+1} + Q_{m-1})}{\sum_m Q_m} - 2g_1 \cos^2 k \frac{\sum_m Q_m^3 (Q_{m+1}^2 + Q_{m-1}^2)}{\sum_m Q_m}. \quad (5.4)$$

We suppose that $Q_m > 0$, $m \in Z$ and $|g_1| \ll 1$. Then, the staggered state lies above the phonon band, while the unstaggered state lies below. We further note that when $\lambda \rightarrow 0$, $|g_1| \rightarrow \infty$. In this case, there is no localized state, staggered or unstaggered, below the phonon band if $g_1 < 0$, or above the phonon band for $g_1 > 0$.

The next important point is the effective mass of unstaggered and staggered localized states[21, 31]. For this we consider the Hamiltonian, $H_{\rm eff}$ given by Eq.(4.5). This consideration will allow us to obtain expressions for the effective mass for almost unstaggered and almost staggered states along with the fully unstaggered and fully staggered localized states[21]. To calculate the effective mass of nearly unstaggered localized states, we let $k \rightarrow 0$ in Eq.(4.5). This in turn yields

$$\lim_{k \rightarrow 0} H_{\rm eff}(x,k,\mu) \sim \frac{1}{2} m_{\rm eff}^{-1}(x) k^2 - 2 A_0(\mu) - 4g_1 A_1(\mu) + 8g_1 A_2(\mu) \cos 2\pi x + O(k^4), \quad (5.5)$$

where we define

$$m_{\rm eff}^{-1}(x) = 2 A_0(\mu) + 8 g_1 A_1(\mu) - 16 g_1 A_2(\mu) \cos 2\pi x \quad (5.6)$$

and A_0, A_1, and A_2 are already defined in the text(see Eq.(4.7)). We note that $m_{\rm eff}(x)$ is even function of both μ and x. It is to be noted that because of the proposed spatial dependence of $m_{\rm eff}$, this is a generalized definition of the quantity. It can be easily seen that for g_1 positive semidefinite, $m_{\rm eff}(x)$ is positive definite for $\mu \in [-\infty, \infty]$. So, when the coupling constant, $g_1 \geq 0$, the effective mass of unstaggered and nearly unstaggered states is positive definite.

To obtain the effective mass of staggered localized states, we put $k = \pi - \theta$ and then let $\theta \rightarrow 0$. This procedure gives

$$-m_{\rm eff}^{-1}(x) = 2 A_0(\mu) - 8 g_1 A_1(\mu) - 16 g_1 A_2(\mu) \cos 2\pi x. \quad (5.7)$$

Consequently, we get from Eq.(5.7) that when $\mu \rightarrow 0$, $m_{\rm eff}^{-1}(x) \rightarrow -2$. On the other hand, in the limit $\mu \gg 1$, the asymptotic form of Eq.(5.7) is

$$- m_{\rm eff}^{-1}(x) \sim \frac{\exp[\mu]}{\mu} [1 - 2 g_1 \exp[\mu] - 2g_1 \frac{\exp[\mu]}{\mu}(1 + 2\cos 2\pi x)]. \quad (5.8)$$

Let us assume that $2 g_1 = \exp[-(1-\epsilon)\mu]$, $\epsilon > 0$ and $\epsilon \mu \rightarrow 0$. We then see from Eq.(5.8) that $m_{\rm eff}(x)$ changes sign. So, depending on the value of g_1, there will be a critical value of μ, $\mu_{\rm cr}(g_1)$, such that for $\mu > \mu_{\rm cr}(g_1)$, staggered as well as nearly staggered localized states will have positive effective mass. For a more precise analy-

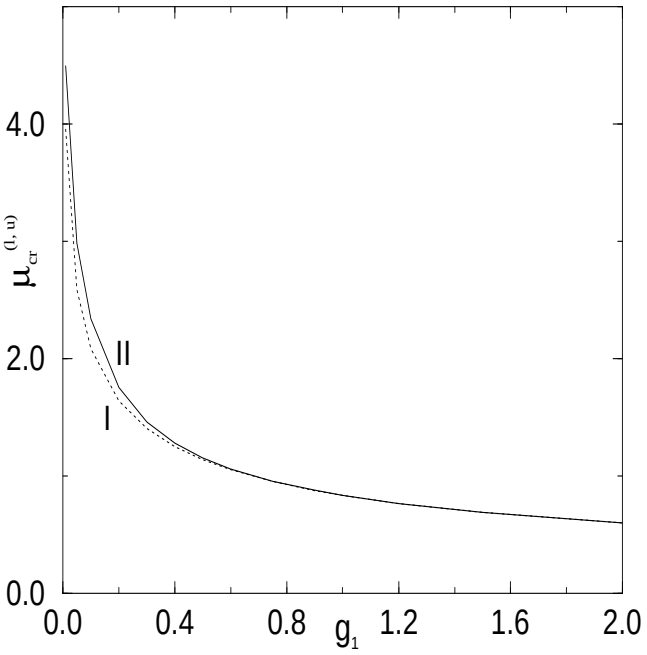

FIG. 5: This shows the variation of $\mu_{\rm cr}^{\rm l}$ and $\mu_{\rm cr}^{\rm u}$ as a function of g_1. Curves I and II respectively. These critical points determine the signature of the effective mass of staggered localized states. Eq(5.7) in the text.

sis of the effective mass, we note that Eq.(5.7) has two critical values of μ, namely $\mu_{\rm cr}^{\rm l}$, and $\mu_{\rm cr}^{\rm u}$, depending on whether $\cos 2\pi x = 1$ or -1. Again, these two critical values of μ move to each other as g_1 increases. This result is indeed substantiated by the numerical analysis of Eq.(5.7) as shown in Fig.5. It is again to note that for $\mu > \mu_{\rm cr}^{\rm u}$, the effective mass is positive definite, while for $\mu < \mu_{\rm cr}^{\rm l}$, the effective mass is negative definite. This in turn implies that the system will have a strongly localized staggered state for $|\mu| > |\mu_{\rm cr}^{\rm l}(g_1)|$. We further note from Eq.(3.1) that μ^{-1} gives the measure of the localization length. So, states for which $\mu \to 0$ in Eq.(3.1) have long localization lengths. We conclude from this analysis then that stationary staggered localized states in the vicinity of upper phonon band edge will have negative effective mass.

VI. A NUMERICAL STUDY OF EQ.(2.5)

A. A study of soliary wave like solutions

For the purpose of numerical integration, we first replace Ψ_m, $m = 1, 2, 3, \cdots$ by $\Psi_m \exp(-2i\tau)$ in Eq.(2.5). Next we write $\Psi_m = \Psi_{1m} + \Im\, \Psi_{2m}$. From Eq.(2.5), we then get

$$
\begin{aligned}
-\dot{\Psi}_{1m} &= (1+\Psi_{1m}^2 + \Psi_{2m}^2)[(\Psi_{2(m+1)} + \Psi_{2(m-1)}) + 2\sum_{j=1}^{l} g_j \{(\Psi_{1m}\Psi_{1(m+j)} \\
&+ \Psi_{2m}\Psi_{2(m+j)})\Psi_{2(m+j)} + (\Psi_{1m}\Psi_{1(m-j)} + \Psi_{2m}\Psi_{2(m-j)})\Psi_{2(m-j)}\}] \qquad (6.1)\\
\dot{\Psi}_{2m} &= (1+\Psi_{1m}^2 + \Psi_{2m}^2)[(\Psi_{1(m+1)} + \Psi_{1(m-1)}) + 2\sum_{j=1}^{l} g_j \{(\Psi_{1m}\Psi_{1(m+j)} \\
&+ \Psi_{2m}\Psi_{2(m+j)})\Psi_{1(m+j)} + (\Psi_{1m}\Psi_{1(m-j)} + \Psi_{2m}\Psi_{2(m-j)})\Psi_{1(m-j)}\}]. \qquad (6.2)
\end{aligned}
$$

For the initial condition, we use[8]

$$\Psi_{1m}(\tau = 0) = \frac{\sinh\mu}{\cosh m\mu}\cos km \qquad (6.3)$$

$$\Psi_{2m}(\tau = 0) = \frac{\sinh\mu}{\cosh m\mu}\sin km. \qquad (6.4)$$

The Fourth order Runge-Kutta method is used to integrate these equations. The chosen time interval for all calculations is 10^{-4}. Furthermore, Eq.(2.4) with $\lambda = 1$ is used to check the accuracy of the integration. In this study an one dimensional lattice, comprising of 257 lattice points with unit lattice spacing is used. The initial condition is centered about the middle of the lattice, that is about the 129th site. For the numerical analysis, we consider two cases, namely (i) $l = 1$ and (ii) $l = 2$ but $g_1 = 0$ in Eq.(2.5). For all cases that are presented in this section $\mu = 1$ and $g_j = 0.5$, $j = 1, 2$.

We note that in the first case the permissible values of k are $\pm\frac{\pi}{2}$ while for the second these values are $\pm\frac{\pi}{4}$ and $\pm\frac{3\pi}{4}$. For the first case the absolute amplitude of the solitary wave like solution (Q_m, see Eq.(3.1)) as a function of site and time (m, τ) is shown in Fig.6 for $k = \frac{\pi}{2}$. Furthermore, for this case the time evolution of the absolute amplitude of the solitary wave ($Q_m(\tau)$) for some arbitarily chosen sites, m are shown in curves I, II, III in Fig.7. For the second case $k = -\frac{3\pi}{4}$ is chosen and the space-time evolution of the $Q_m(\tau)$ is shown in Fig.8. We note that in all cases the initial profile moves undistorted.

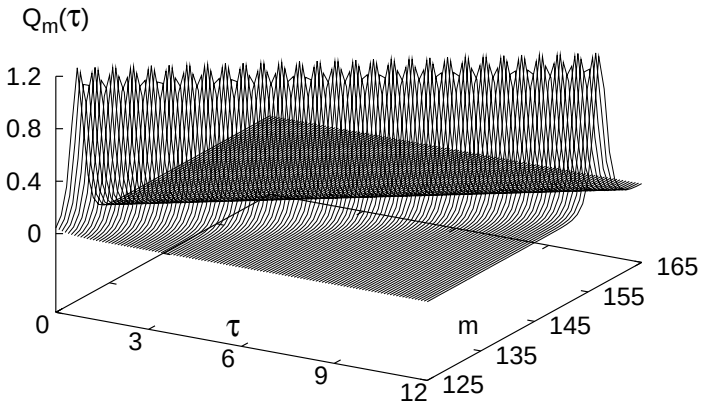

FIG. 6: The N-AL dynamics of an initial Ablowitz-Ladik soliton with $k = \frac{\pi}{2}$, Eq.(2.5). Furthermore, $l = 1$, $g_1 = 0.5$ and $\mu = 1.0$. The number of sites in the chain is 257 and the origin is taken at the center of the chain.

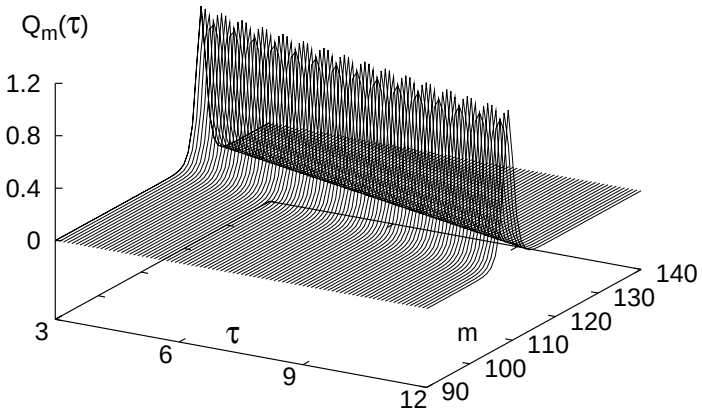

FIG. 8: The N-AL dynamics of an initial Ablowitz-Ladik soliton with $k = -\frac{3\pi}{4}$, Eq.(2.5). Furthermore, $l = 2$, $g_1 = 0.0$, $g_2 = 0.5$ and $\mu = 1.0$. The number of sites in the chain is 257 and the origin is taken at the center of the chain.

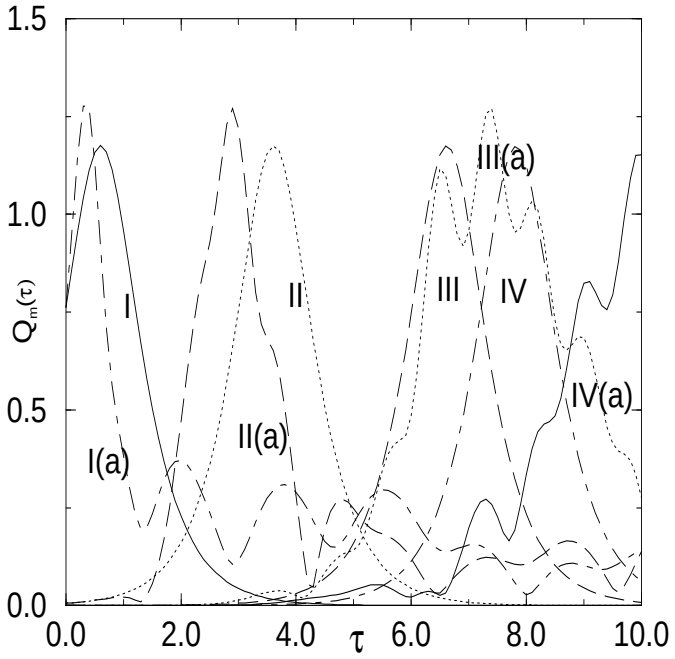

FIG. 7: The N-AL equation (Eq.(2.5)) determined time evolution of $Q_m(\tau)$ (Eq.(3.1)) for some chosen values of sites, m . $k = \frac{\pi}{2}$, and $\frac{\pi}{3}$ respectively. For both cases $l = 1$, $g_1 = 0.5$ and $\mu = 1.0$. The number of sites in the chain is 257 and the origin is taken at the center of the chain. I, I(a): $m = 130$, II, II(a): $m = 140$, III, III(a): $m = 150$. The (a) series is for $k = \frac{\pi}{3}$ while the other one is for $k = \frac{\pi}{2}$.

These pictures are expectedly identical to the space-time evolution of the pure A-L solitons. This is also verified by numerical integration.

B. A study of the PN pinning of solitary waves

Another important aspect that we study numerically here is the effect of PN potential, which arises due to the nonintegrability term in Eq.(2.5) on the space-time evolution of the initial profile given by Eq.(6.3) and Eq.(6.4)[31, 41]. We note that the nonintegrability effect is maximum when $k = 0$ in Eq.(3.1). On the other hand it totally vanishes at $|k| = \frac{\pi}{2}$ for $l = 1$. We study again the propagation of an initial profile for $l = 1$, but with $\mu = 1.0$ and $g_1 = 0.5$. The accuracy of the integration is checked by the constancy of $\mathcal{N}$(Eq.(2.4)). It is found that the loss of constancy becomes more and more discernible as $||k| - \frac{\pi}{2}| \to \frac{\pi}{2}$. This makes the simulation for small values of k less reliable. Fig.9 shows the space-time evolution of $Q_m(\tau)$ (Eq.(3.1)) for $k = \frac{\pi}{3}$. We note that the dispersion and the distortion of the initial profile is very transparent in the figure (Fig.9). For better understanding, we also show through curves I(a) to III(a) in Fig.7 and I(a) to IV(a) in Fig.10 the time evolution of the $Q_m(\tau)$ for some arbitrarily chosen site or m values for $k = \frac{\pi}{3}$ and $\frac{\pi}{4}$ respectively. We note that the distortion of the initial profile and the intensity of the phonon tail increase as k decreases from

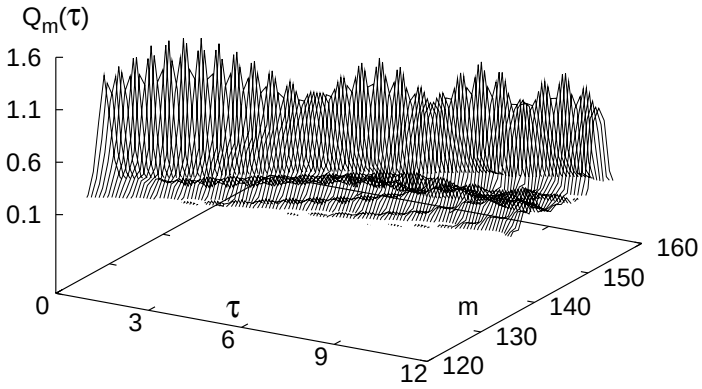

FIG. 9: The N-AL dynamics of an initial Ablowitz-Ladik soliton with $k = \frac{\pi}{3}$, Eq.(2.5). Furthermore, $l = 1$, $g_1 = 0.5$ and $\mu = 1.0$. The number of sites in the chain is 257 and the origin is taken at the center of the chain.

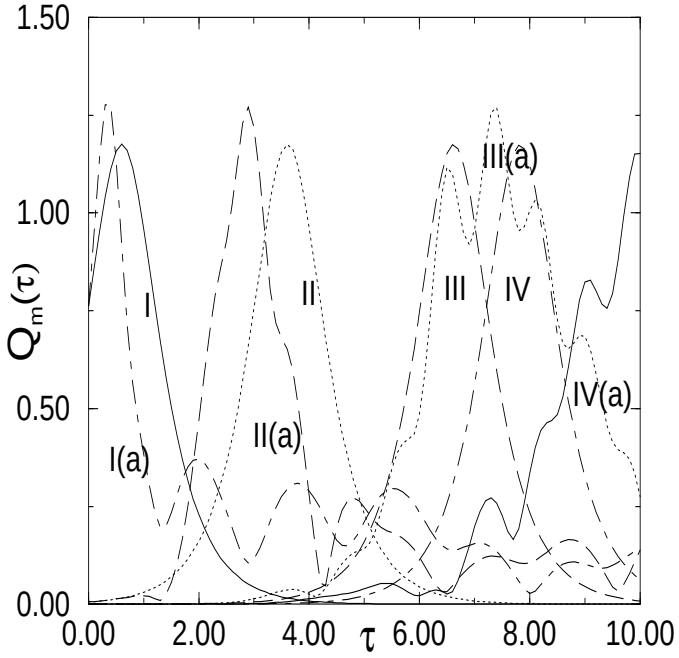

FIG. 10: Same as Figure 7, but with $k = \frac{\pi}{4}$ for both cases. I, I(a): $m = 130$, II, II(a): $m = 135$, III, III(a): $m = 140$, IV, IV(a): $m = 142$. While (a) series is for the N-AL equation, the other one is for the Ablowitz-Ladik soliton.

$\frac{\pi}{3}$ to $\frac{\pi}{4}$. This is, of course in the expected direction. Furthermore, in both cases the initial profile slows down by leaving phonon behind in the propagation. Through curves I to IV in Fig.10 the time evolution of $Q_m(\tau)$ for same values of m from the Ablowitz-Ladik equation are included for comparison. This slowing down is very transparent in the figure (Fig.10). So, it is reasonable to assume that these moving profiles will ultimately be trapped. However, we do not observe the total trapping in our simulations. We possibly need large integrability breaking term to see the total trapping in the time of simulations. In case of $k = \frac{\pi}{2}$, the nonintegrability term in Eq.(2.5) vanishes, and expectedly the initial profile (Eq.(6.3) and Eq.(6.4)) propagates undistorted without any change in its speed and leaving no phonon tail behind as can be seen in Fig.6 and curves I to III in Fig.7.

C. A study of interaction of two solitary waves

An important and also extensively studied field in nonlinear dynamics is the investigation and the understanding of interaction of two or more solitary waves of nonintegrable nonlinear equations and the components of vector solitons in integrable nonlinear equations. So far only continuous nonlinear nonintegrable equations are studied[30, 33, 34, 35, 36, 37, 38, 43, 44]. This is due to the nonavailability of any discrete nonlinear equation having solitary wave like solutions. In this context, therefore, the N-AL equation (Eq.(2.5)) that is proposed here assumes a very great significance. This equation gives us the opportunity for the first time to study the interaction of solitary waves of a discrete nonlinear equation. To investigate this problem, as the initial condition we take the function[35, 36]

$$\Psi_m(0) \;=\; \frac{f_1 \sinh\mu}{\cosh[\mu(m-x_0)]}\exp[ik_1(m-x_0] \;+\; \frac{f_2\sinh\mu}{\cosh[\mu(m+x_0)]}\exp[ik_2(m+x_0]. \tag{6.5}$$

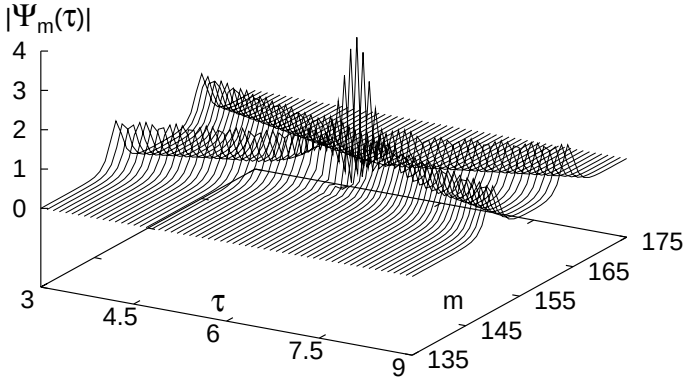

FIG. 11: The N-AL collision dynamics of two initial A-L pulses. $k_2 = -k_1 = \frac{\pi}{2}$. $l = 1$, $g_1 = 0.5$ and $\mu = 1.0$ as mentioned in the text. The number of sites in the chain is 313 and the origin is taken at the middle of the chain.

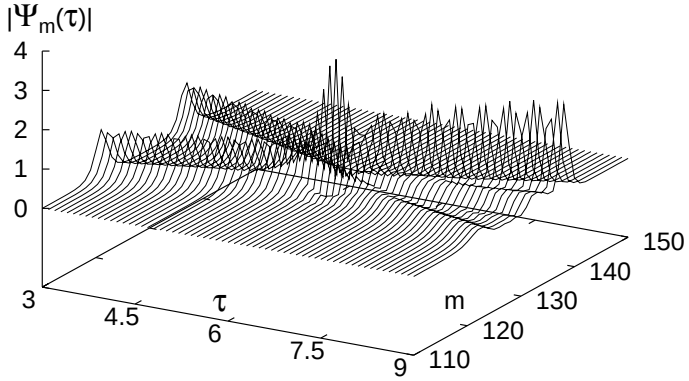

FIG. 12: Same as in Fig.11, but with $k_1 = \frac{\pi}{2.05}$, and $k_2 = -\frac{\pi}{2}$. $l = 1$, $g_1 = 0.5$, and $\mu = 1.0$. In this simulation, the number of sites is 257.

We note that the function has two peaks at $x = x_0$ and $x = -x_0$ respectively. The velocity of the peak at x_0 is $\frac{\sinh\mu}{\mu}\sin k_1$ while the velocity of the other peak at $x = -x_0$ is $\frac{\sinh\mu}{\mu}\sin k_2$. We further note that when $|x_0| \rightarrow \infty$, Eq.(6.5) gives two A-L type solitons (Eq.(3.1)). This analysis is also done numerically using the fourth order Runge-Kutta method, and the origin is placed at the center of the one dimensional chain. For all studies, we take $2|x_0| = 30$ units, and $f_1 = f_2 = 1.0$

The first one is as usual the $l = 1$ case. For this analysis we take for all cases $\mu = 1.0$ $g_1 = 0.5$. Inasmuch as $|k| = \frac{\pi}{2}$ in Eq.(3.1) is an exact one soliton solution of Eq.(2.5) , we consider first the case $k_2 = -k_1 = \frac{\pi}{2}$. In this case, we find that two peaks emerge after the collision without any change in shape and without any emission of phonon (see also ref.34). Of course, there can be phase shifts in these peaks after collision, but this is not investigated. This case of collision of solitons is shown in Fig.11. We further note that the result is found to be independent of the value of g_1. But, we did not check the effect of changing μ on the collision. The other case that is considered is $k_1 = -\frac{\pi}{2.05}$ and $k_2 = \frac{\pi}{2}$. When $g_1 = 0$, we find that two solitons collide and after the collision again two peaks emerge without any change in shape and without any emission of phonon. This is not shown here. On the other hand, when we give a non-zero value of g_1 (in our case 0.5), we find the fusion of two solitons on collision. Inasmuch as $k_2 = \frac{\pi}{2}$, the direction of the maximum velocity is in the direction of increasing lattice sites. The fused solution expectedly moves in that direction. But, at the same time it emits phonons, as shown in Fig.12[33].

The second case that we study is the case of $l = 2$, but $g_1 = 0.0$. In this case we have four permissible values of k, namely $k = \pm\frac{3\pi}{4}$, and $\pm\frac{\pi}{4}$. Of course, there are only two velocities, just like the previous one. However, if choose k_1 and k_2 from these allowed values of k, for $|x_0| \rightarrow \infty$, Eq.(6.5) will be the solution of Eq.(2.5). In this analysis, we choose $\mu = 1.5$, $g_2 = 0.5$, and $2|x_0| = 30$ units. For this case the space-time evolution of a solitary wave with $k = -\frac{3\pi}{4}$ is already shown in Fig.8. In the first case we take $k_1 = -k_2 = -\frac{3\pi}{4}$ and the numerical simulation is shown in Fig.13. In this cae we see that two solitary waves do not pass each other. On the other hand after coming close to each other, they are repelled. Other cases that are studied are $k_1 = -\frac{\pi}{4}$, but $k_2 = \frac{3\pi}{4}$, and$k_1 = -\frac{3\pi}{4}$, but $k_2 = \frac{\pi}{4}$

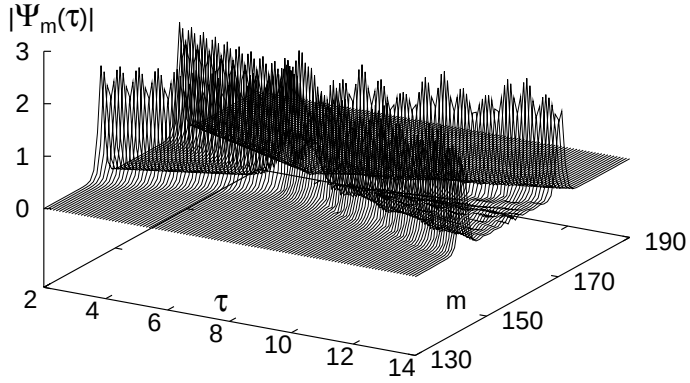

FIG. 13: The N-AL collision dynamics of two initial A-L pulses. $k_2 = -k_1 = \frac{3\pi}{4}$. $l = 2$, $g_1 = 0.0$, $g_2 = 0.5$ and $\mu = 1.5$ as mentioned in the text. The number of sites in the chain is 313 and the origin is taken at the middle of the chain.

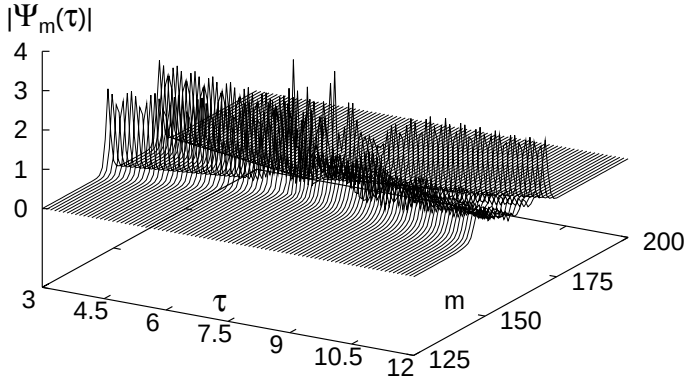

FIG. 14: Same as in Fig.13, but with $k_1 = -\frac{\pi}{4}$, and $k_2 = \frac{3\pi}{4}$. $l = 2$, $g_1 = 0.0$, $g_2 = 0.5$, and $\mu = 1.5$. In this simulation, the number of sites is 313.

respectively. Our numerical simulations for these cases are shown in Fig.14 and Fig.15 respectively. In the first case, we see that two solitary waves fuse after collision and then move in the direction of positive velocity simultaneously emiting phonons. In the second case, however, we see the total destruction of the initial profile, Eq.(6.5) after the collision. This implies that there is no definite pattern in the collision process. Furthermore, the result of collision appears to be very sensitive to the phases of the colliding solitary waves. So, there should be attempts to understand this collision physics analytically, using perturbative method and collective coordinate method[37]

VII. SUMMARY

A new class of nonintegrable Hamiltonians with tunable nonlinearities is propsed here to derive a class of (1 + 1) dimensional nonintegrable discrete nonlinear Schrödinger equations, which include both some known nonlinear equations such as Ablowitz-Ladik nonlinear Schrödinger equation[6, 7], IN-DNLS[31, 45, 46] and a new subset, collectively christened as the N-AL equation(Eq.(2.5)). The relevant equations are obtained from the proposed Hamiltonian by the standard procedure of classical mechanics, but by employing a standard generalized definition of Poisson brackets, as shown in the Appendix A below. In this paper two cases of the N-AL

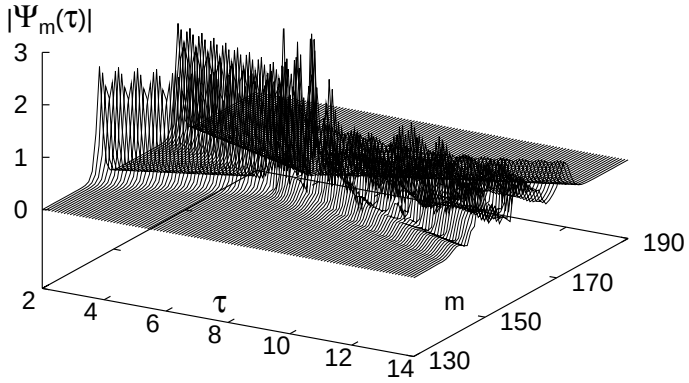

FIG. 15: Same as in Fig.14, but with $k_1 = -\frac{3\pi}{4}$, and $k_2 = \frac{\pi}{4}$. $l = 2$, $g_1 = 0.0$, $g_2 = 0.5$, and $\mu = 1.5$. In this simulation, the number of sites is 313.

equation are investigated analytically as well as numerically. These cases are $(i)\ l = 1$, and $(ii)\ l = 2$, but $g_1 = 0.0$ in Eq.(2.5).

An important characteristic of the N-AL equation is shown to be that it can allow spatially localized states of A-L type (Eq.(3.1)) for certain permissible values of the parameter k to travel without distortion and without emiting phonons. This is found both analytically as well as numerically. So, these special solutions have in them the required balance of the nonlinearity and dispersion[5] and also are transparent to the PN potential arising from the lattice discreteness[31, 41]. The transparency of these solutions to the PN potential proves that these have the *continuous* translational symmetry of the one-soliton solution of the Ablowitz-Ladik equation (Eq.(3.1))[31].

Trapped and moving solitons are found from Eq.(2.5). This analysis is done using a standard perturbative procedure[21, 22]. The most interesting part of this analysis, however, is that it shows the existence of *saddle center bifurcations*. This in turn implies the presence of minimum energy breathers in the system. Breathers are by definition time periodic, spatially localized solutions of equations of motion for classical degrees of freedom interacting on a lattice[54]. We note that eq.(4.1) satisfy these requirements. Since, the saddle center bifurcation is seen in the perturbative method, it is, therefore, imperative to study the existence of breathers in the system numerically. We further note that in this system we also find a chain of centers. The origin of this situation is explained in the text. One interesting consequence of this occurence is phase portraits showing relaxation oscillations in regions, which are physically forbidden parts of the phase space for this system. Since phase portraits are very rich in characteristics, it is worthwhile to study them quite elaborately by varying extensively parameters, such as μ and g_1 and and also including more terms in $S(\mu, x)$ (Eq.(4.1).

The presence of stable localized states in Eq.(2.5) is also investigated, albeit a more systematic analysis, presumably by the discrete variational method is required. This work is indeed in progress. The effective mass of localized states are analyzed here using the effective Hamiltonian, given by Eq.(4.5)[21]. It is found that nearly unstaggered as well as unstaggered localized states will always have positive effective mass. On the other hand, nearly staggered and staggered localized states can have both negative and positive effective depending on the value of μ in Eq.(3.1). However, large width but small amplitude nearly staggered and staggered localized states do have the expected negative effective mass.

It is further shown here numerically that all other solitary wave profiles (Eq.(6.3) and Eq.(6.4)) under the dynamics described by Eq.(2.5) and for which the nonintegrable term in Eq.(2.5) does not vanish, suffer distortion and emit phonons in the propagation. Further investigations along this line by altering the strength of the nonintegrable term by altering the value of k reveal that the extent of distortion and the extent of emission of phonons by the initial solitary wave profiles (Eq.(6.3) and Eq.(6.4)) depend on the magnitude of the nonintegrable term. We conclude from these two findings that any general solitary wave profile due to the presence of the nonintegrable term in Eq.(2.5) is subjected to both the dynamical imbalance between the nonlinearity and the dispersion, and to the PN potential. We note that the continuous translational symmetry of these solitary wave profiles breaks down due to the nonintegrable term in Eq.(2.5). Consequently, these profiles scan the lattice discreteness in the propagation. This, in turn implies that the moving profiles experience the effect of PN potential in the dynamics. Since, any general solitary wave profile suffers from these two factors, we expect that the profile can either be trapped by emiting phonons or the localized structure will spread uniformly due to the effect of extra dispersion. Notwithstanding the slowing down of initial profiles are observed in our simulations, our numerical study in this matter, however, is not conclusive. So, a more elaborate study increasing the coupling constants in the nonintegrable term in Eq.(2.5) and also changing the parameter μ in Eq.(3.1) is needed. This will be done in future.

Finally, the N-AL equation (Eq.(2.5))is the discrete analog of the famous ϕ^4 equation, however with an important difference, that this equation only gives dynamical solitary wave like solutions. None the less, the importance of the N-AL equation in this regard cannot be overlooked. This equation gives the opportunity for the first time to study the collision dynamics of solitary wave profiles using a discrete nonlinear nonintegrable equation. Here only the collision of two solitary wave profiles are studied (Eq.(6.5)). In this study we find that at least the interaction of two solitary wave profiles have some universal features, meaning that the outcome does not depend critically on the nature of the nonlinear equation. It is also equally true that we do not find so far any systematic pattern in the dynamics. It is, therefore, necessary to study this problem in details both analytically and numerically to discern if there is any specific pattern in the dynamics. Another imporatnt aspect to study is the fractal structure of the emeging profile after the collision as a function of the initial velocity and the strength of the nonintegrable term[37, 38].

We conclude by noting that this study offers a very significant insight into the transport properties of the DHM. Furthermore, the N-AL equation can be used to study transport properties of localized states in soft molecular chains, having the coexsistence of nonlinearity and disorder, nolinearity and quasiperiodicity or incommesurabily in various parameters, such as the hopping integral, J and the nonintegrable coupling constants , $g_j,\ j = 1, 2, \cdots$. Furthermore, the aplicability of the N-AL equation in the study exciton dynamics in photosynthesis and in molecular solids should be explored.

APPENDIX A: GENERALIZED POISSON BRACKET

We consider a dynamical system having 2 N generalized coordinates, $\{\phi_n,\ \phi_n^\star\}$, $n\ =\ 1,\ \ldots N$. Let U and V be any two general dynamical variables of the system. We now define a nonstandard Poisson bracket[2]

$$\{U,\ V\}_{\{\phi,\ \phi^\star\}}\ =\ \sum_{n\ =\ 1}^{N}\ (\frac{\partial U}{\partial \phi_n}\ \frac{\partial V}{\partial \phi_n^\star} - \frac{\partial V}{\partial \phi_n}\ \frac{\partial U}{\partial \phi_n^\star})\ (1 + \lambda\ |\phi_n|^2). \tag{A1}$$

When $U\ =\ \phi_m$ and $V\ =\ \phi_l^\star$, we then have [21, 31, 57]

$$\{\phi_m,\ \phi_l^\star\}_{\{\phi,\ \phi^\star\}}\ =\ (1\ +\ \lambda\ |\phi_m|^2)\ \delta_{ml}. \tag{A2}$$

From Eq.(A1) we further have for $\{m,\ l\}$

$$\{\phi_m,\ \phi_l\}_{\{\phi,\ \phi^\star\}}\ =\ \{\phi_m^\star,\ \phi_l^\star\}_{\{\phi,\ \phi^\star\}}\ =\ 0. \tag{A3}$$

Then when $U\ =\ \phi_m$ and $V\ =\ \mathrm{H}$, we have from Eq.(A1)

$$\{\phi_m, \mathrm{H}\}_{\{\phi,\ \phi^\star\}}\ =\ (1\ +\ \lambda\ |\phi_m|^2)\ \frac{\partial \mathrm{H}}{\partial \phi_m^\star}. \tag{A4}$$

We then write for the dynamical evolution of the m-th generalized coordinate, ϕ_m[31, 57]

$$i\ \frac{d\phi_m}{dt}\ =\ \{\phi_m, \mathrm{H}\}_{\{\phi,\ \phi^\star\}}\ =\ (1\ +\ \lambda\ |\phi_m|^2)\ \frac{\partial \mathrm{H}}{\partial \phi_m^\star}. \tag{A5}$$

This is consistent because

$$\begin{aligned} i\ \frac{dU}{dt}\ &=\ \sum_{n\ =\ 1}^{N}\ (\frac{\partial U}{\partial \phi_n}\ i\ \dot{\phi_n}\ +\ \frac{\partial U}{\partial \phi_n^\star}\ i\ \dot{\phi_n^\star}) \\ &=\ \sum_{n\ =\ 1}^{N}\ (1\ +\ \lambda\ |\phi_n|^2)\ (\frac{\partial \mathrm{U}}{\partial \phi_n}\ \frac{\partial \mathrm{H}}{\partial \phi_n^\star}\ -\ \frac{\partial \mathrm{U}}{\partial \phi_n^\star}\ \frac{\partial \mathrm{H}}{\partial \phi_n}) \\ &=\ \{U,\ \mathrm{H}\}_{\{\phi,\ \phi^\star\}}. \end{aligned} \tag{A6}$$

We note now that when $U\ =\ \mathrm{H}$, we have $\frac{d\mathrm{H}}{dt}\ =\ 0$. In other words, H is a constant of motion. Consider $\mathcal{N}$ given by Eq.(2.4). To show that it is a constant of motion, we write $\mathrm{H}\ =\ \mathrm{H}_0\ +\ \mathrm{H}_1\ -\ \frac{2}{\lambda}(\frac{\nu}{\lambda}\ - J)\ \mathcal{N}$, where we define

$$\mathrm{H}_0\ =\ J\ \sum_n\ (\phi_n^\star\ \phi_{n+1}\ +\ \phi_{n+1}^\star\ \phi_n)\ +\frac{2\nu}{\lambda}\ \sum_n |\phi_n|^2, \tag{A7}$$

$$\mathrm{H}_1\ =\ -\ \frac{1}{2}\ \sum_n\ \sum_{j\ =\ 1}^{l}\ g_0^j\ (\phi_n^\star\ \phi_{n+j}\ +\ \phi_{n+j}^\star\ \phi_n)^2. \tag{A8}$$

We then find that

$$i\ \frac{d\mathcal{N}}{dt}\ =\ \lambda\ \sum_n [(\phi_n^\star\ \frac{\partial \mathrm{H}_0}{\partial \phi_n^\star} - \phi_n\ \frac{\partial \mathrm{H}_0}{\partial \phi_n}) + (\phi_n^\star\ \frac{\partial \mathrm{H}_1}{\partial \phi_n^\star} - \phi_n\ \frac{\partial \mathrm{H}_1}{\partial \phi_n})]. \tag{A9}$$

By using (A7) and (A8), it is very simple to show that the right hand side of (A9) is zero. Hence, $\mathcal{N}$ is a constant of motion.

[1] P. G. Drazin and R. S. Johnson, *Solitons : an introduction* (Cambridge Univ. Press, Cambridge, 1989).

[2] A. Scott, *Nonlinear Science : Emergence & Dynamics of Coherent Structures*, (Oxford University Press, U. K. 1999).

[3] See e. g. M. Remoissenet, *Waves Called Solitons : Concepts and Experiments* (Springer-Verlag, Berlin, 1996).

[4] Yu. S. Kivshar and B. A. Malomed, Rev. Mod. Phys. **63**, 761, (1989).

[5] R. Z. Sagdeev, S. S. Meiseev, A. V. Tur and V. V. Yanevskii, *Nolinear Phenomena in Plasma Physics and Hydrodynamics*, ed. R. Z. Sagdeev, (Mir Publishers, Moscow), 137 (1986).

[6] M. J. Ablowitz and P. A. Clarkson, *Solitons, Nonlinear Evolution Equations and Inverse Scattering* (Cambridge Univ. Press, Cambidge, 1991).

[7] M. J. Ablowitz and J. L. Ladik, J. Math. Phys. **16**, 598, (1975), *ibid*, **17**, 1011, (1976).

[8] S. Takeno and S. Homma, J. Phys. Soc. Jpn, 60, 731 (1991).

[9] E. W. Laedke, K. H. Spatschek and S. K. Turitsyn, Phys. Rev. Lett. **73**, 1055 (1994).

[10] A. Ghosh, B. C. Gupta and K. Kundu, J. Phys. : Condens. Matter, **10**, 2701 (1998).

[11] K. Kundu and B. C. Gupta, Eur. Phys. J. B **3** 23 (1998); B. C. Gupta and K. Kundu, *Nonlinear Dynamics: Integrabilty and Chaos* Eds. M. Daniel, K. M. Tamizhmani and R. Sahadevan, p. 193 (Narosa, New Delhi, 2002)

[12] V. E. Zakharov and A. B. Shabat, Zh. Eksp. Teor. Fiz. **61**, 118 (1971), [Sov. Phys. JETP **34**, 62 (1972)].

[13] A. S. Davydov and N. I. Kislukha, Zh. Eksp. Teor. Fiz. **71**, 1090 (1976), [Sov. Phys. JETP **44**, 571 (1976)].

[14] A. C. Scott, Phys. Rev. A **26**, 578 (1982)

[15] A. Scott, *Davydov's Soliton*, Phys. Rep. **217**, 3 (1992).

[16] J. C. Bronski, L. D. Carr, B. Deconinck and J. N. Kutz, Phys. Rev. Lett. **86**, 1402 (2001), A. Trombettoni and A. Smerzi, Phys. Rev. Lett. **86**, 2353 (2001).

[17] I. V. Barashenkov and E. V. Zemlyanaya, Phys. Rev. Lett. **83**, 2568 (1999).

[18] Ch. Claude, Y. S. Kivshar, O. Kluth and K. H. Spatchek, Phys. Rev. B **47**, 14228 (1993).

[19] A. B. Aceves, C. De Angelis, T Peschel, R. Muschall, F. Lederer, S. Trillo and S. Wabnitz, Phys. Rev. E **53**, 1172 (1996).

[20] S. Yomosa, J. Phys. Soc. Jpn. **52**, 1866 (1983).

[21] K. Kundu, Phys. Rev. E, **61**, 5839 (2000).

[22] A. A. Vakhnenko and Yu. B. Gaididei, Theo. Math. Fiz. **68**, 350 (1986) [Theor. Math. Phys. **68**, 873 (1987)].

[23] S. Takeno, J. Phys. Soc. Jpn. **61**, 1433 (1992).

[24] K. Hori and S. Takeno, J. Phys. soc. Jpn. **61** 4263 (1992).

[25] V. V. Konotop and S. Takeno, Phys. Rev. B **55**, 11342 (1997).

[26] Yu. S. Kivshar, D. E. Pelinovsky, T. Cretegny and M. Peyard, Phys. Rev. Lett. **80**, 5032 (1998).

[27] A. S. Davydov, Zh. Eksp. Teor. Fiz. **78**, 789 (1980) [Sov. Phys. JETP **51**, 397 (1980)].

[28] H. Bolterauer, *Davydov's soliton revisited, self- trapping of vibrational energy in protein*, eds. P. L. Christeinsen and A. C. Scott, NATO ASI series, Vol. **234**, 309 (1990).

[29] W. Förner and J. Ladik, *Davydov's soliton revisited, self-trapping of vibrational energy in protein*, eds. P. L. Christeinsen and A. C. Scott, NATO ASI series, Vol. **234**, 267 (1990).

[30] S. V. Dmitriev, Yu. S. Kivshar and T. Shigenari, Phys. Rev. Lett., **64**, 056613 (2001).

[31] D. Cai, A. R. Bishop, N. Grønbech-Jensen, Phys. Rev. Lett. **72**, 591 (1994).

[32] M. Johansson and Yu. S. Kivshar, Phys. Rev. Lett. **82**, 85 (1999).

[33] R. K. Bullough and P. J. Caudrey, *Topics in Current Physics : Solitons*, Eds. R. K. Bullough and P. J. Caudrey, p. 6 (Springer-Verlag, Berlin, 1980).

[34] S. Aubry, J. Chem. Phys. **64**, 3392 (1976).

[35] A. E. Kudryavtsev, Pis'ma Zh. Eksp. Teor. Fiz. **22**, 178 (1975), [JETP Lett., **22**, 82 (1975)].

[36] B. S. Getmanov, Pis'ma Zh. Eksp. Teor. Fiz. **24**, 323 (1976), [JETP Lett. **24**, 291 (1976)].

[37] P. Anninos, S. Oliveira and R. A. Matzner, Phys. Rev. D **44** 1147 (1991).

[38] J. Yang and Yu Tan, Phys. Rev. Lett. **85**, 3624 (2000), Phys. Lett. A **280**, 129 (2001), Yu Tan and J. Yang, Phys. Rev. E. **64**, 056616 (2001).

[39] D. H. Dunlop, H-L Wu and P. Phillips, Phys. Rev. Lett. **65**, 88 (1990).

[40] K. Kundu, D. Giri and K. Ray, J. Phys. A : Math Gen. **29**, 5699 (1996).

[41] Y. S. Kivshar and D. K. Campbell, Phys. Rev. E **48**, 3077 (1993).

[42] S. Takeno, *Davydov's soliton revisited, self- trapping of vibrational energy in protein*, eds. P. L. Christeinsen and A. C. Scott, NATO ASI series, Vol. **234**, 31 (1990).

[43] G. I. Stegeman and M. Segev, Science, **286**, 1518 (1999), M. Segev and G. Stegeman, *Physics Today*, 42 (August, 1998).

[44] T. Kanna and M. Lakshmanan, Phy. Rev. Lett. **86**, 5043 (2001), C. Anastassiou, M. Segev, K. Steiglitz, J. A. Giordmaine and M. Mitchell, Phys. Rev. Lett. **83**, 2332 (1999).

[45] M. Salerno, Phys. Rev. A **46**, 6856 (1992).

[46] V. V. Konotop and M. Salerno, Phys. Rev. E **55**, 4706 (1997), *ibid* **56**, 3611 (1997).

[47] E. I. Rashba, in *Excitons* eds. E. I. Rashba and M. D. Sturge (North Holland Publ, Amsterdam, 1982).

[48] Y. Toyozawa, In *Molecular Aggregates Springer series in Solid- State Sciences*. 49, eds. P. Reineker, H. Haken and H. C. Wolf (Springer-Verlag, Berlin, 1983).

[49] H. van Amerongen, L. Valkunas and R. van Grondelle, *Photosynthetic EXCITONS*, Chap. 6, pp.197-240, (World Scientific, Singapore, 2000).

[50] D. I. Kaup, SIAM J. Appl. Math. **31**, 121 (1976).

[51] D. K. Arrowsmith and C. M. Place, *Ordinary Differential Equations*, (Chapman and Hall, London, 1982).

[52] K. T. Alligood, T. D. Sauer and J. A. Yorke, *Chaos: an introduction to dynamical systems*, (Springer-Verlag, New York, 1997).

[53] P. G. Drazin, *Nonlinear Systems*, (Cambridge University Press U. K. 1992).

[54] S. Flach, K. Kladko, and R. MacKay, Phys. Rev. Lett. **78**, 1207 (1997).

[55] B. Meerson and G. I. Shinar, Phys. Rev. E **56**, 256 (1997).

[56] E. C. Zeeman, *Differential Equations for the Heartbeat and Nerve Impulse*, Salvador Symposium on Dynamical Systems, Academic Press, pp. 683-741.

[57] A. Das, *Integrable Models*, (World Scientific, Singpore, 1989).